DOI: 10.17725/rensit.2020.12.437

Optimization of a Polarization Nephelometer

Viktor G. Oshlakov, Anatoly P. Shcherbakov
V.E. Zuev Institute of Atmospheric Optics SB RAS, http://www.iao.ru/
Tomsk 634055, Russian Federation
E-mail: oshlakov@iao.ru, molnija2@inbox.ru

Yaroslav A. Ilyushin
Lomonosov Moscow State University, https://www.msu.ru/
Moscow 119991, Russian Federation
E-mail: ilyushin@physics.msu.ru.

Received June 01, 2020; peer-reviewed June 29, 2020; accepted July 06, 2020

Abstract: **The effect of parameters of a polarization nephelometer on its accuracy characteristic is analyzed. Errors in approximation of the actual scattering volume and actual optical beam by the elementary scattering volume and elementary beam are considered. A five-wave monochromatic source of radiation with the high spectral intensity of 0.15÷0.6 W is described. The design of polarization units is demonstrated.**

Keywords: **polarization, nephelometer, non-isotropic scatterer, scattering matrix, elementary vol-ume, elementary optical beam, approximation error, LED, encoder, microprocessor, precision position control, pulse width modulation, PID controller**

UDC 535.36+530.1

Acknowledgements: The authors are thankful to N.N. Bakin, the head of division of Scientific Research Institute of High-Precision Devices, for consultation concerning application of modern LEDs. This study has been accomplished within the framework of State Assignment of IAO SB RAS.

For citation: Viktor G. Oshlakov, Anatoly P. Shcherbakov, Yaroslav A. Ilyushin. Optimization of a Polarization Nephelometer. *RENSIT,* 2020, 12(4):437-450. DOI: 10.17725/rensit.2020.12.437.

Contents

1. INTRODUCTION

The scattering matrix (D_{mn}), $m,n = \overline{1,4}$, relates the Stokes vector of the incident radiation $\mathbf{S}_s$ to the Stokes vector **S** of the radiation scattered by a small volume *dv* at an angle φ with respect to the incident radiation (**Fig. 1**). The scattering matrix for radiation of the optical wavelength range is used in problems of optical wave propagation, laser sensing, polarization filtering, and others. In the general case of a nonisotropic medium, it is impossible to predetermine identical and zero elements of the scattering matrix. That is why all 16 elements of the matrix (D_{mn}), $m,n = \overline{1,4}$., are to be determined. The importance and complexity

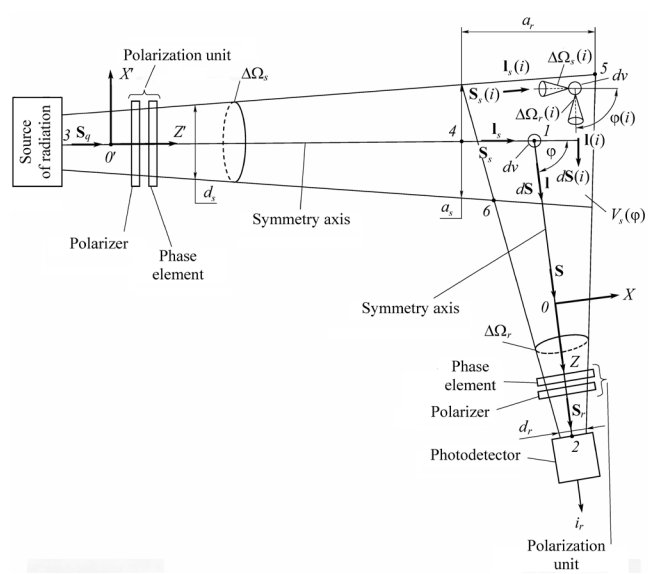

Fig. 1. *Block diagram of goniometer of the polarization nephelometer.*

of making a device that automatically measures the matrix (D_{mn}), $m,n = \overline{1,4}$., were indicated in [1]. This problem is solved methodologically in [2, 3]. An optimal meter of the scattering matrix needs in the proper calibration. The modulation method of measuring the scattering matrix, which was used, for example, in [4, 5], cannot be applied in the laser sensing. Theoretical studies have shown that in the case of an isotropic medium, identical and zero elements of the matrix D can be predetermined. The measurements of the matrix D in [4, 5] employ these results. Consequently, the technique [4, 5] is applicable only in isotropic media. The technique for measuring the matrix of any medium that was proposed in [2, 3] is applicable to laser sensing as well. The achieved level of development of microprocessor technology makes it possible to accomplish completely the task specified in [1].

The scattering volume of a polarization nephelometer and an optical beam incident on the scattering volume should be elementary. However, only qualitative definitions of these terms are known. That is why the paper considers the approximation of the actual scattering volume and the actual optical beam by the elementary ones.

A monochromatic source with high spectral intensity required for polarization measurements can be created using high-brightness LEDs. The analysis of parameters of the polarization nephelometer will allow improvement of its accuracy and size characteristics.

2. OPTIMIZATION OF DIMENSIONS OF A POLARIZATION NEPHELOMETER

Write the Stokes vector **S** of radiation in the form

$$d\mathbf{S} = (IQUV)^T, \quad (1)$$

where T is the transposition sign. Then, the Stokes vector $d\mathbf{S} = (dI(i)dQ(i)dU(i)dV(i))^T$ of radiation scattered by the small volume dv (Fig. 1) being at some point i of the scattering medium at the observation point spaced by $r(i)$ from the scattering volume is [1]

$$d\mathbf{S}(i) = \frac{1}{r^2(i)} D(\varphi(i), \mathbf{I}_s(i), \mathbf{I}(i))\mathbf{S}_s(i)dv, \quad (2)$$

where $\mathbf{S}_s(i) = (I_s(i)Q_s(i)U_s(i)V_s(i))^T$ is the Stokes vector of the optical beam incident on the volume dv; this beam propagates within the small solid angle $d\Omega_s(i)$ and its axis is described by the direction vector $\mathbf{I}_s(i)$; $\mathbf{S}(i)$ is the Stokes vector of the optical beam of scattered radiation; it propagates within the small solid angle $\Delta\Omega(i)$ and its axis is described by the direction vector $\mathbf{I}(i)$; $\varphi(i)$ is the angle between the vectors $\mathbf{I}_s(i)$ and $\mathbf{I}(i)$. We adhere to the notation of the parameters I,Q,U,V of the Stokes vector **S** as in [2,3].

In the case of a non-isotropic medium, the elements of the matrix $D(\varphi(i), \mathbf{I}_s(i), \mathbf{I}(i))$ are functions of the position of the scattering plane described by the vectors $\mathbf{I}_s(i)$ and $\mathbf{I}(i)$ and the angle $\varphi(i)$. To measure the matrix $D(\varphi, \mathbf{I}_s, \mathbf{I})$ in the open range $\varphi = (0°, 180°)$, the polarization nephelometer constructed by the goniometer scheme [4,5] (Fig. 1) is used. The radiation source generates an optical beam with the diameter d_s (diameter is understood as the maximal cross section size) and divergence $\Delta\Omega_s$. In the course of propagation, the radiation passes successively the polarization unit (PU) of the radiation source. The polarization unit consists of a polarizer and a phase element. The radiation should be maximally monochromatic for the optical path difference of its orthogonal components at the exit of the phase element to be constant. A photodetector with the entrance pupil diameter d_r and the field-of-view divergence $\Delta\Omega_r$ receives the radiation upon the successive passage of the PU phase element and polarizer. The symmetry axes of the optical beam emitted by the source and the photodetector field of view are given by the direction vectors $\mathbf{I}_s$ and **I**, respectively. The symmetry axes intersect at point 1. The photodetector should turn around the axis passing through this point and perpendicular

to the plane defined by the vectors $\mathbf{I}_s$ and $\mathbf{I}$. The angle φ between the vectors $\mathbf{I}_s$ and $\mathbf{I}$ defines the scattering angle of the matrix $D(\varphi, \mathbf{I}_s, \mathbf{I})$, while the vectors themselves define the scattering plane. In [6,7], a single photodetector rotating around the axis is replaced with five photodetectors installed at different angles φ.

The sum of the distances between the points 1, 2 (A_r) and 1, 3 (A_s) is called the nephelometer base A.

Examples of some nephelometers used in experiments in the isotropic atmosphere are given in **Table 1**.

As can be seen from Table 1, the nephelometers differ widely in the values of the parameters A, d_r, and d_s. The ranges of applicability of these nephelometers with respect to atmospheric parameters are discussed insufficiently. The issue of optimization of nephelometer parameters from the viewpoint of improvement of its accuracy characteristics has received insufficient attention as well.

The descriptions of nephelometers often include the concepts of the elementary volume $V_{se1}(\varphi)$ and the elementary optical beam, which are some idealizations of the actual volume $V_s(\varphi)$ and the actual beam. However, the accuracy of approximation of the actual parameters by the elementary volume $V_{se1}(\varphi)$ and the elementary beam was not discussed yet.

The scattering volume $V_s(\varphi)$ (Fig. 1) is bounded by the lateral surfaces of the optical beam emitted by the radiation source and the photodetector field of view. It is characterized by the cross-section diameters of the optical beam a_s and the photodetector field of view a_r.

Table 1

Parameters of nephelometers

Parameter	Reference		
	[4]	[6]	[7]
Base A, м	8	0.58	0.58
d_s, м	0.2	0.03	0.03
d_r, м	0.1	0.03	0.03
Divergence of optical beam emitted by source	40'	40'	40'
Divergence of photodetector field of view	2÷4°	3°	3°

For the small volume dv at point 1, Eq. (2) has the form

$$d\mathbf{S} = \frac{1}{A_r^2} D(\varphi, \mathbf{I}_s, \mathbf{I})\mathbf{S}_s dv. \quad (3)$$

Introduce the right coordinate systems XYZ and $X'Y'Z'$ with the axes X,Z and X',Z' lying in the scattering plane determined by the vectors $\mathbf{I}_s$ and $\mathbf{I}$, which are at the same time the direction vectors of the axes Z' and Z, respectively. The vectors $\mathbf{S}_s$ and $d\mathbf{S}$ will be determined relative to the axes X' and X, respectively.

The main task of a polarization nephelometer is to determine matrix $D(\varphi, \mathbf{I}_s, \mathbf{I})$ elements (in absolute units) satisfying Eq. (3). The volume should be large enough for we can believe that it includes the complete set of all particles characteristic of this medium. In the case of well mixed "clear" air containing aerosol particles with the size of few micrometers near the Earth's surface, the volume can be taken equal to few cubic centimeters. The same is also true for moderately dense, but stable stratiform clouds. However, in the case of dense cumulus clouds, the volume of 1 cm^3 is sufficient to determine reliably the size distribution function and concentration of particle [8]. The small volume is a volume of the scattering medium containing the general set of particles.

Let the volume $V_s(\varphi)$ contain N small volumes dv and let every i-th volume dv have some point i, the right coordinate systems $X(i)Y(i)Z(i)$ and $X'(i)Y'(i)Z'(i)$ are anchored to. The axes $Y(i)$ and $Y'(i)$ are perpendicular to the scattering plane at the point i of the i-th volume dv, which is determined by the vectors $\mathbf{I}_s(i)$ and $\mathbf{I}(i)$ coinciding with the axes of optical beams of the incident and scattered radiation of the i-th volume dv, respectively. The directions of the axes $Z(i)$ and $Z'(i)$ coincide with those of the vectors $\mathbf{I}(i)$ and $\mathbf{I}_s(i)$. The vectors $\mathbf{S}_s(i)$ and $d\mathbf{S}(i)$ of, respectively, the incident and scattered radiation of the i-th volume dv are determined relative to the axes $X'(i)$ and $X(i)$.

The distance A_r should always exceed (no less than fivefold) the diameter of any cross

section of the volume $V_s(\varphi)$ by the plane perpendicular to the axis of the photodetector field of view [12]. In addition, the photodetector PU should not fall within the volume $V_s(\varphi)$. The requirement for the distance between points 1 and 6 of the volume $V_s(\varphi)$ to be no larger than A_r at the angle

$$\varphi = \begin{cases} \varphi_{\min}, \text{ at } \varphi_{\min} < 10^\circ, \\ 10^\circ, \text{ at } \varphi_{\min} > 10^\circ, \end{cases}$$

where $[\varphi_{\min}, \varphi_{\max}]$ is the angular range of measurement of the matrix D, satisfies this condition. Consequently, the following condition should be true:

$$A_r > \frac{dr}{2} ctg \frac{\varphi}{2}, \tag{3a}$$

where

$$\varphi = \begin{cases} \varphi_{\min}, \text{ at } \varphi_{\min} < 10^\circ, \\ 10^\circ, \text{ at } \varphi_{\min} > 10^\circ, \end{cases}$$

It is assumed that for $V_s(\varphi) \le V_{se1}(\varphi)$ at the distance A_r fulfilling Eq. (3a) with allowance made for Eq. (3), we can write with a small error

$$S = \frac{1}{A_r^2} \int_{V_s(\varphi)} D(\varphi, \mathbf{I}_s, \mathbf{I}) \mathbf{S}_s(i) dv \cong$$
$$\cong \frac{1}{A_r^2} D(\varphi, \mathbf{I}_s, \mathbf{I}) \mathbf{S}_s V_s(\varphi), \tag{4}$$

where $D(\varphi, \mathbf{I}_s, \mathbf{I})$ is the scattering matrix of the volume dv, $\mathbf{S}_s(i)$ is the Stokes vector of the optical beam incident onto this volume, and $\mathbf{S}_s$ is the Stokes vector of the optical beam irradiating the volume $V_s(\varphi)$.

Equation (4) is valid when the intensity of the radiation incident on the volume $V_s(\varphi)$ remains practically constant within this volume. In the volume $V_{se1}(\varphi)$, the amount of the absorbed and scattered radiation is proportional to the volume [9]. The propagation of radiation in a scattering medium is accompanied by multiple scattering. In the radiation incident on the volume $V_s(\varphi)$, the fraction of the multiply scattered radiation should be negligibly small in comparison with the direct radiation. An isotropic medium can be characterized by the extinction coefficient $k_\lambda = \alpha + \sigma$, where α is the absorption coefficient, σ is the scattering coefficient. In this case, the optical thickness $\tau(A_s) = k_\lambda A_s$ and $\tau(a_s) = k_\lambda a_r$ should not exceed 5 to 6 [1].

Consider the approximation of the volume $V_s(\varphi)$ of an isotropic medium by the volume $V_{se1}(\varphi)$.

The optical flux Φ_s of unit power upon the propagation of the path l decreases by Φ_{ext} equal to

$$\Phi_{ext} = 1 - e^{-\tau(l)} =$$
$$= \tau(l) - \frac{\tau(l)^2}{2!} + \frac{\tau(l)^3}{3!} - \ldots - \frac{(-\tau(l))^n}{n!} = \tag{5}$$
$$= \tau(l) - \tilde{\tau}(l),$$

where

$$\tau(l) = k_\lambda l,$$
$$\tilde{\tau}(l) = \frac{\tau(l)^2}{2!} - \frac{\tau(l)^3}{3!} + \ldots + \frac{(-\tau(l))^n}{n!}.$$

It follows from Eq. (5) that if the optical thickness $\tau(a_r)$ (Fig. 1) of the volume $V_s(\varphi)$ fulfills the condition

$$\tau(a_r) \gg \tilde{\tau}(a_r), \tag{6}$$

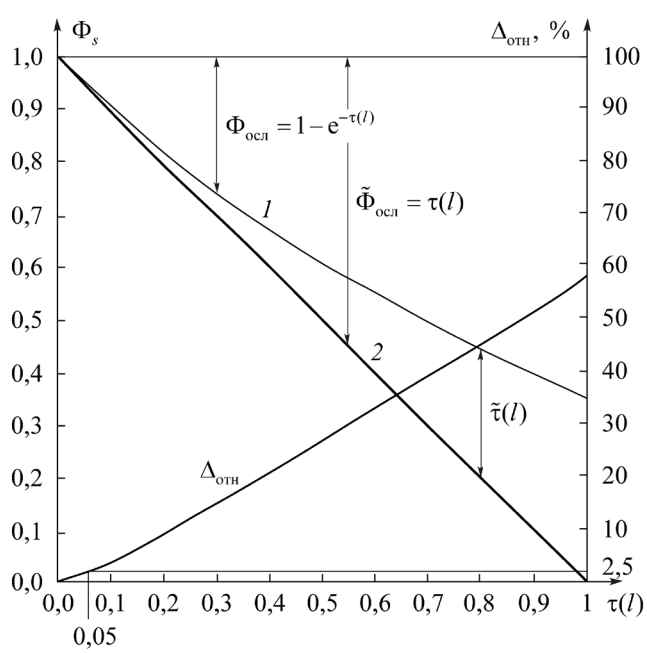

Fig. 2. *Extinction of optical beam of unit power by an actual volume $V_s(\varphi)$ (1) and an elementary volume $V_{se1}(\varphi)$ (2), relative error Δ_{rel}(%) of approximation of the actual volume by the elementary volume.*

then it can be considered as the volume $V_{se1}(\varphi)$ with some error. **Fig. 2** demonstrates the extinction of the optical beam Φ_s of unit power by the volume $V_s(\varphi)$ (line 1) and by its approximation by the volume $V_{se1}(\varphi)$ (line 2). The relative error of this approximation Δ_{rel} can be determined as

$$\Delta_{rel} = \frac{\tilde{\Phi}_{ext} - \Phi_{ext}}{\Phi_{ext}}, \tag{7}$$

where $\tilde{\Phi}_{ext} = \tau(l)$ is the extinction of unit-power flux by the volume $V_{se1}(\varphi)$.

The thickness a_r of the volume $V_s(\varphi)$, whose optical thickness if $\tau(a_r) = 0.05$, can be taken as that of the volume $V_{se1}(\varphi)$ with the error Δ_{rel} = 2.5%.

This criterion allows us to determine $a_r = 0.05/k_\lambda$. The volume, whose thickness a_r for the optical beam is

$$a_r < 0.05/k_\lambda, \tag{8}$$

can be taken as the volume $V_{se1}(\varphi)$.

Practically any volume $V_s(\varphi)$ of the sufficiently homogeneous medium contains the large number of scattering and absorbing centers. Therefore, the condition of statistical representativeness of an elementary volume, whose optical thickness is $\tau(a_r) = 0.05$, is always fulfilled with high accuracy. That is why the thickness a_r of the volume dv can be much smaller than $0.05/k_\lambda$.

Using the Koschmieder formula, we can rewrite Eq. (8) as

$$a_r = 0.013L_{MVR}, \tag{9}$$

where L_{MVR} is the meteorological visibility range.

ASSUMPTION 1. Matrix $\tilde{D}_{mn}$, $m,n = \overline{1,4}$, measured by the polarization nephelometer is the matrix (D_{mn}), $m,n = \overline{1,4}$, of the medium, if in the volume $V_s(\varphi)$ the scattering planes of all small volumes dv determined by the vectors $\mathbf{I}_s(i)$ and $\mathbf{I}(i)$ are parallel and the angles $\varphi(i)$ between them are identical.

Assumption 1 is satisfied, if Items 1 or 2 are satisfied.

1. The scattering volume $V_s(\varphi)$ is contracted to the volume dv at point 1.
2. The optical beam emitted by the radiation source at the length a_r can be approximated by the elementary beam with a small error, and the photodetector 2 field-of-view angle α_r in the scattering plane is small.

The optical beam with the small value of relative change in the brightness at the distance a_r can be substituted by the elementary optical beam with a small error. If the optical beam from the radiation source propagates in the solid angle $\Delta\Omega_s$, then the brightness of the optical beam L_s irradiating the volume $V_s(\varphi)$ at point 4 is

$$L_s = \frac{E^{\perp}}{\Delta\Omega_s} = \frac{4I}{\pi a_s^2}, \tag{10}$$

where $E^{\perp}$ is the illuminance in the cross section of the beam, I is the luminous intensity.

The relative change of brightness δL_s at the distance a_r is

$$\delta L_s = \frac{L_s - L_s(a_r)}{L_s(a_r)} = \frac{L_s}{L_s(a_r)} - 1, \tag{11}$$

where $L_s(a_r)$ is brightness of the optical beam at the distance a_r from point 4.

With Eq. (10), we can write a decrease in brightness $\delta = L_s/L_s(a_r)$ in the form

$$\delta = \frac{L_s}{L_s(a_r)} = \frac{2(a_s/2 + a_r tg\alpha_s)^2}{a_s^2} = \\ = 1 + \frac{2a_r tg\alpha_s}{a_s}\left(1 + \frac{2a_r}{a_s} tg\alpha_s\right), \tag{12}$$

where $2L_s$ is the divergence of the optical beam.

With allowance made for Eq. (12), the value of δL_s is

$$\delta L_s = \frac{2a_r tg\alpha_s}{a_s}\left(1 + \frac{2a_r}{a_s} tg\alpha_s\right). \tag{13}$$

The value of δL_s characterizes the relative change in the brightness L_s of the optical beam at the distance a_r and is determined by the parameter $\widetilde{\delta L_s} = \frac{a_r}{a_s} tg\alpha_s$. The parallel optical beam is an ideal representative of an elementary beam, and $\widetilde{\delta L_s} = 0$ in it. At the small distance a_r, δL_s of the beam can be neglected, and the beam itself at this distance can be considered

as an elementary optical beam. Thus, we can believe that the error of approximation of the light beam of a polarization nephelometer with the length a_r by the elementary optical beam is determined by the value of the parameter

$$\widetilde{\delta L}_s = \frac{a_r}{a_s} tg\alpha_s \quad (14)$$

3. OPTIMAL METER OF THE MATRIX D(φ, L_s, L) AND ITS CALIBRATION

The method employed in the optimal meter of the matrix $D(\varphi, \mathbf{I}_s, \mathbf{I})$ allows all elements of the matrix to be determined from separate measurements of the signal i_r at the exit of the photodetector without additional transformations of the signal i_r [2, 3]. The algorithm for control of polarization elements in PUs of the radiation source and the photodetector is optimal, because it provides the smallest errors in measuring the elements of the matrix $D(\varphi, \mathbf{I}_s, \mathbf{I})$ due to inaccuracies in manufacture and installation of polarization elements. At the same time it is easy to implement, because only the position of the fast axis (FA) of the phase elements in PUs of the source and the photodetector is controlled, the discrete number is minimal, and the positions of the fast axes of the phase elements in PUs of the source and the photodetector are independent of elements of the matrix $D(\varphi, \mathbf{I}_s, \mathbf{I})$.

Let the volume $V_s(\varphi)$ satisfy Assumption 1 with a small error, and we can take $(\tilde{D}_{mn}) \cong (D_{mn}),\ \ m,n = \overline{1,4}.$

If the distance $A_r \gg a_s$, but it influence on the value of the vector **S** is negligibly small, then Eq. (4) can be written in the form

$$\mathbf{S} = D(\varphi, \mathbf{I}_s, \mathbf{I})\mathbf{S}_s V_s(\varphi), \quad (15)$$

where $\mathbf{S}_s = (I_s Q_s U_s V_s)^T$, $\mathbf{S} = (IQUV)^T$.

The measurements in the polarization nephelometer should satisfy Eq. (15). To measure 16 elements of the matrix $D(\varphi, \mathbf{I}_s, \mathbf{I})$, 16 independent equations are sufficient. Every vector $\mathbf{S}_s$ corresponds to four equations in Eq. (15), each containing one parameter of the vector **S**. Consequently, to determine 16 elements of the matrix, it is sufficient for the source to generate four types of polarization described by the vectors $\mathbf{S}_{sj} = (I_{sj} Q_{sj} U_{sj} V_{sj})^T, j = \overline{1,4}$ [2,3].

These 16 equations can be written in the form

$$\mathbf{S}_j = (I_j Q_j U_j V_j)^T = D(\varphi, \mathbf{I}_s, \mathbf{I})\mathbf{S}_{sj} V_s(\varphi), j = \overline{1,4} \quad (16)$$

The vector $\mathbf{S}_{sj}$ determined by the vector $\mathbf{S}_q$ and the Mueller matrices of the polarizer and phase element of PU of the radiation source can be written in the form

$$S_{sj} = E\begin{pmatrix} 1 \\ \cos 2\alpha'_j \cos 2(\alpha'_j - \beta') + \cos\tau' \sin 2\alpha'_j \sin 2(\alpha'_j - \beta') \\ \sin 2\alpha'_j \cos 2(\alpha'_j - \beta') - \cos\tau' \cos 2\alpha'_j \sin 2(\alpha'_j - \beta') \\ \sin\tau' \sin 2(\alpha'_j - \beta') \end{pmatrix}, \quad (17)$$

where $E = (1/2)(I_0 + Q_0\cos 2\beta' + U_0 \sin 2\beta')$, and I_0, Q_0, U_0 are the parameters of the vector $\mathbf{S}_0$ of generated radiation (in the presence of a depolarizer, $Q_0 = U_0 = 0$), β' is the angle of orientation of the polarizer transmission plane (TP), α_j' is the angle of orientation of FA of the phase element, which is measured relative to the axis X' (α_j' corresponds to the j-th position of FA, $j = 1, 4$); τ' is the phase shift of orthogonal components of the phase element.

Separate the normalized vector $\mathbf{S}_{ij}$ from the vector $\mathbf{S}_{ij}$ given by Eq. (17)

$$\tilde{S}_{sj} = \begin{pmatrix} 1 \\ Q_{sj} \\ U_{sj} \\ V_{sj} \end{pmatrix} = \begin{pmatrix} 1 \\ \cos 2\alpha'_j \cos 2(\alpha'_j - \beta') + \cos\tau' \sin 2\alpha'_j \sin 2(\alpha'_j - \beta') \\ \sin 2\alpha'_j \cos 2(\alpha'_j - \beta') - \cos\tau' \cos 2\alpha'_j \sin 2(\alpha'_j - \beta') \\ \sin\tau' \sin 2(\alpha'_j - \beta') \end{pmatrix} \quad (18)$$

and rewrite Eq. (16) in the form

$$\mathbf{S}_j = D'(\varphi, \mathbf{I}_s, \mathbf{I})\mathbf{S}_{sj}, j = \overline{1,4} \quad (19)$$

where

$$D'(\varphi, \mathbf{I}_s, \mathbf{I}) = EV_s(\varphi)D(\varphi, \mathbf{I}_s, \mathbf{I}).$$

We use the parameters of the vectors $\mathbf{S}_{sj}, j = \overline{1,4}$ to form the matrix W nondegenerate at any α_j'

$$W = \begin{pmatrix} 1 & Q_{s1} & U_{s1} & V_{s1} \\ 1 & Q_{s2} & U_{s2} & V_{s2} \\ 1 & Q_{s3} & U_{s3} & V_{s3} \\ 1 & Q_{s4} & U_{s4} & V_{s4} \end{pmatrix} \quad (20)$$

and then group system (19) into four systems, each determining a line of the matrix $D'(\varphi, \mathbf{I}_s, \mathbf{I})$:

$$W\mathbf{D}'_1 = \mathbf{I}_W, \; W\mathbf{D}'_2 = \mathbf{Q}_W, \; W\mathbf{D}'_3 = \mathbf{U}_W, \; W\mathbf{D}'_4 = \mathbf{V}_W, \quad (21)$$

where $\mathbf{D}'_m = \mathrm{E}V_s(\varphi)(D_{m1}D_{m2}D_{m3}D_{m4})^{\mathrm{T}}$, $m = \overline{1,4}$; $(D_{m1}D_{m2}D_{m3}D_{m4})$ – is the m-th line of the matrix $D(\varphi, \mathbf{I}_s, \mathbf{I})$; $\mathbf{I}_W = (I_1I_2I_3I_4)^{\mathrm{T}}$, $\mathbf{Q}_W = (Q_1Q_2Q_3Q_4)^{\mathrm{T}}$, $\mathbf{U}_W = (U_1U_2U_3U_4)^{\mathrm{T}}$, $\mathbf{V}_W = (V_1V_2V_3V_4)^{\mathrm{T}}$ – are the vectors composed of the parameters of the vectors $\mathbf{S}_j = (I_jQ_jU_jV_j)^{\mathrm{T}}$, $j = \overline{1,4}$.

For systems (21) W, $\mathbf{I}_W$, $\mathbf{Q}_W$, $\mathbf{U}_W$, and $\mathbf{V}_W$ are input data in the meter of the vectors $\mathbf{D}'_1$, $\mathbf{D}'_2$, $\mathbf{D}'_3$ *and* $\mathbf{D}'_4$. The inaccuracy in determination of the input data in Eq. (21) has the smallest ef-fect on the accuracy of determination of the vectors $\mathbf{D}'_i$, $i = 1,4$, when the conditioning number Cond$W$ of the matrix W is minimal [10]. The conditioning number of the nondegenerate matrix can be determined as

$$CondW = \|W\|\|W^{-1}\|,$$

where $\|...\|$ denotes the norm of the matrix; W^{-1} is the matrix inverse to the matrix W.

The choice of some or other particular norm is dictated by the requirements imposed on the accuracy of solution. The choice of the Euclidian norm corresponds to the criterion of smallness of the root-mean-square error.

In the optimal meter, the minimal conditioning number Cond$W$ of the matrix W obeying the Euclidian norm of the matrix is equal to 4.4722 at the position of FA of the phase element deter-mined by the angles α'_1 = 38.54°; α'_2 = 75.14°; α'_3 = 105.38°; α'_4 = 141.857°, the phase shift τ' = 131.795°, and the angle of orientation of the polarizer TP β' = 90°. The parameters τ', α'_j, $j = \overline{1,4}$, and β' should be measured with high accuracy, and the Mueller matrices of polarization elements should differ only slightly from the Mueller matrices of ideal polarization elements.

The photodetector can measure only the parameter I_r of the vector $\mathbf{S}_r = (I_rQ_rU_rV_r)^T$ through measurement of the signal $i_r = \psi I_r$, where ψ is the photodetector sensitivity. The vector $\mathbf{S}_r$ is determined by the vector $\mathbf{S}$ and the Mueller matrices of the phase element and the polarizer of the photodetector PU.

To measure the parameters $IQUV$ of the vector $\mathbf{S}$, four independent equations obtained through the measurement of the parameter I_r at each of the four positions of FA of the phase element of photodetector PU are sufficient. These equations have the form

$$I_{ri} = \frac{1}{2}(m_{i1}I + m_{i2}Q + m_{i3}Y + m_{i4}V), \; i = \overline{1,4}, \quad (22)$$

where

$m_{i1} = 1$; $m_{i2} = \cos2\alpha_i\cos2(\alpha_i - \beta) + \cos\tau\sin2\alpha_i\sin2(\alpha_i - \beta)$;

$m_{i3} = \sin2\alpha_i\cos2(\alpha_i - \beta) - \cos\tau\cos2\alpha_i\sin2(\alpha_i - \beta)$;

$m_{i4} = -\sin\tau\sin2(\alpha_i - \beta)$;

i is the serial number of the position of FA of the phase element; α_i is the angle of orientation of FA of the phase element corresponding to the i-th position, β is the angle of orientation of TP of the polarizer of photodetector PU relative to the axis X; τ is the phase shift of orthogonal compo-nents of the phase element.

The matrix (m_{in}), $i, n = \overline{1,4}$, of the system of equation (22) is denoted as M. This matrix differs from the matrix W given by Eq. (20) by the sign of the elements in the fourth column. Therefore, the minimal conditioning numbers of these matrices are Cond$M$ = Cond$W$ = 4.4722.

In the meter of the vector $\mathbf{S}$, the input data are I_{ri}, $i = \overline{1,4}$, and the matrix M. In the optimal meter of the vector $\mathbf{S}$, the minimal value Cond$M \le 1.53$ is achieved at the position of FA of the phase element determined by the angles α'_1 = 38.54°; α'_2 = 75.14°; α'_3 = 105.38°; α'_4 = 141.857°, the phase shift τ' = 131.795°, and angle of orientation of the polarizer TP β' = 90°. The parameters τ', α'_j, $j = \overline{1,4}$, and β' should be measured with high accuracy, and the Mueller matrices of the polarization elements should be

close to the Mueller matrices of ideal polarization elements.

Let I_{rij} be the value of the parameter I_r of the vector $\mathbf{S}_r$ at the j-th position of FA of the phase element of PU of the radiation source and i-th position of FA of the phase element of the photodetector PU. Then, it follows from Eq. (22) that

$$\mathbf{S}_j = 2M^{-1}\mathbf{I}_{rij}, \quad i = \overline{1,4}, \tag{23}$$

where $\mathbf{I}_{rij} = (I_{r1j} I_{r2j} I_{r3j} I_{r4j})^{\mathrm{T}}$, $M^{-1} = (\tilde{m}_{in})$, $i, n = 1,4$ is the matrix inverse to the matrix M.

Introduce the matrix E, whose elements are determined by the photodetector signal $i_{rij} = \psi I_{rij}$

$$E = \begin{pmatrix} i_{r11} & i_{r21} & i_{r31} & i_{r41} \\ i_{r12} & i_{r22} & i_{r32} & i_{r42} \\ i_{r13} & i_{r23} & i_{r33} & i_{r43} \\ i_{r14} & i_{r24} & i_{r34} & i_{r44} \end{pmatrix}. \tag{24}$$

Then, with allowance made for Eqs. (21), (23), and (24), we have

$$\begin{aligned} \mathbf{D}'_1 &= W^{-1}\mathbf{I}_W = \frac{2}{\psi} W^{-1} E \tilde{\mathbf{m}}_{1n}, \; n = \overline{1,4}, \\ \mathbf{D}'_2 &= W^{-1}\mathbf{Q}_W = \frac{2}{\psi} W^{-1} E \tilde{\mathbf{m}}_{2n}, \; n = \overline{1,4}, \\ \mathbf{D}'_3 &= W^{-1}\mathbf{U}_W = \frac{2}{\psi} W^{-1} E \tilde{\mathbf{m}}_{3n}, \; n = \overline{1,4}, \\ \mathbf{D}'_4 &= W^{-1}\mathbf{V}_W = \frac{2}{\psi} W^{-1} E \tilde{\mathbf{m}}_{4n}, \; n = \overline{1,4}, \end{aligned} \tag{25}$$

where $\tilde{\mathbf{m}}_{in} = (\tilde{m}_{i1}\tilde{m}_{i2}\tilde{m}_{i3}\tilde{m}_{i4})^T$; $(\tilde{m}_{i1}\tilde{m}_{i2}\tilde{m}_{i3}\tilde{m}_{i4})$ is the i-th line of the matrix M^{-1}.

In the general case, Eq. (25) can be written as

$$\mathbf{D}_i = \frac{1}{K(\varphi)} 2W^{-1} E \tilde{\mathbf{m}}_{in}, \; n = \overline{1,4}, \tag{26}$$

where $\mathbf{D}_i^T = (D_{i1}D_{i2}D_{i3}D_{i4})$; $(D_{i1}D_{i2}D_{i3}D_{i4})$ is the i-th line of the matrix $D(\varphi, \mathbf{I}_s, \mathbf{I})$; $\tilde{\mathbf{m}}_{in}^T = (\tilde{m}_{i1}\tilde{m}_{i2}\tilde{m}_{i3}\tilde{m}_{i4})$; $(\tilde{m}_{i1}\tilde{m}_{i2}\tilde{m}_{i3}\tilde{m}_{i4})$ is the i-th line of the matrix M^{-1}; $K(\varphi) = EV_s(\varphi)\psi$ is the calibration coefficient.

The control over the discrete positions of the phase elements can be the following:

1. FA of the phase element of PU of the radiation source is successively set to the position $j = \overline{1,4}$.
2. At each position j of FA of the phase element of PU of the radiation source, the signal i_{rij}, $i = \overline{1,4}$, is measured through discrete setting FA of the phase element of the photodetector to the position $i = \overline{1,4}$.

Thus, at each position of FA of the phase element of PU of the radiation source, the j-th line of the matrix E is determined. Execution of Items 1 and 2 and Eq. (25) determines the matrix $\psi D'(\varphi, \mathbf{I}_s, \mathbf{I}) = K(\varphi)D(\varphi, \mathbf{I}_s, \mathbf{I})$.

Using Eq. (25), we can write the element $EV_s(\varphi)\psi D_{11}$ necessary for the calibration in the form $EV_s(\varphi)\psi D_{11} = \tilde{D}_{11}$, where

$$\begin{aligned} \tilde{D}_{11} = 2[&\tilde{w}_{11}(i_{r11}\tilde{m}_{11} + i_{r21}\tilde{m}_{12} + i_{r31}\tilde{m}_{13} + i_{r41}\tilde{m}_{14}) + \\ &+\tilde{w}_{12}(i_{r12}\tilde{m}_{11} + i_{r22}\tilde{m}_{12} + i_{r32}\tilde{m}_{13} + i_{r42}\tilde{m}_{14}) + \\ &+\tilde{w}_{13}(i_{r13}\tilde{m}_{11} + i_{r23}\tilde{m}_{12} + i_{r33}\tilde{m}_{13} + i_{r43}\tilde{m}_{14}) + \\ &+\tilde{w}_{14}(i_{r14}\tilde{m}_{11} + i_{r24}\tilde{m}_{12} + i_{r34}\tilde{m}_{13} + i_{r44}\tilde{m}_{14})] \end{aligned} \tag{27}$$

is the relative value of the element D_{11} of matrix $D(\varphi, \mathbf{I}_s, \mathbf{I})$.

The matrix D can be calculated from one system of 16 equations, whose right-hand sides are the parameters $I_{rij} = i_{rij}/\psi$ [3]. Let us form the vector

$$I_{rij} = (I_{r11}...I_{r14}I_{r21}...I_{r24}I_{r31}...I_{r34}I_{r41}...I_{r44})^T.$$

These systems of equations in the matrix form can be represented as:

$$B\mathbf{D}_{mn} = \mathbf{I}_{rij},$$

where $D_{mn} = (D_{11}...D_{14}D_{21}...D_{24}D_{31}...D_{34}D_{41}...D_{44})^T$ and D_{ij} are elements of the matrix $D(\varphi, \mathbf{I}_s, \mathbf{I})$; $B = M \otimes W$ is the Kronecker (direct) multiplication of the matrices M and W.

Using the equation [10]:

$$\|M\|_E = \sqrt{S_p M^T M},$$

where $\|M\|_E$ is the Euclidian norm of the matrix M and SpM^TM is the spur (trace) of the matrix M^TM, we can obtain

$$CondB = \| B \|_E \| B^{-1} \|_E = CondMCondW. \tag{28}$$

Consequently, *CondB* achieves the minimum when *CondM* and *CondW* determined from the positions of FA of the phase elements of PUs of the source and the photodetector achieve the minima. The values of *CondM* and *CondW*, which provide for the minimum, are independent of the elements of the matrix $D(\varphi, \mathbf{I}_s, \mathbf{I})$ and absolutely optimal.

The aim of the calibration is to determine the calibration coefficient $K(\varphi) = EV_s(\varphi)\psi$.

The method of calibration with the use of a diffusively reflecting (diffusively transmitting) screen in the non-polarized radiation from a source is described in [11]. This method is most correct, because it takes into account the geometric configuration of the volume $V_s(\varphi)$ and irregular illuminance of its points. In the optimal meter of the matrix $D(\varphi, \mathbf{I}_s, \mathbf{I})$, the source radiation is fully polarized. Therefore, the method [11] should be modified to be used in the optimal meter of the matrix $D(\varphi, \mathbf{I}_s, \mathbf{I})$.

The ideal diffusively reflecting (diffusively transmitting) screen has the following properties:

(a) all the incident radiation is reflected (or transmitted) by the screen surface;

(b) the screen brightness is identical in all directions;

(c) the reflected (transmitted) radiation is non-polarized in all directions.

If the surface of an actual diffusively reflecting (diffusively transmitting) screen has the illuminance E, then its brightness L regardless of polarization of the incident radiation is

$$L = \beta \frac{E}{\pi},$$

where β is the brightness coefficient of the diffusively reflecting (diffusively transmitting) screen. The brightness coefficient β is understood as a ratio of the brightness of this screen in some direction to the brightness of an ideal screen being under the same illuminance conditions. If a surface coated by an MgO layer is illuminated normally and observed at the angle $\xi \approx 30°$ to the normal, then $\beta = 1$ and the brightness is $L = E/\pi$ (Fig. 3) [12].

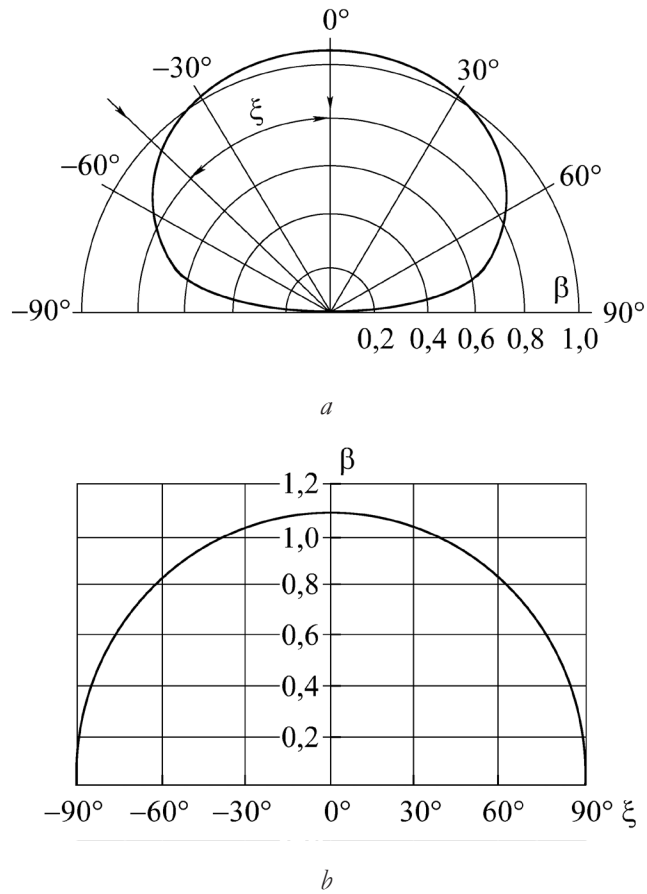

Fig. 3. *Brightness coefficients in the scattering MgO surface in polar (a) and orthogonal (b) coordinates.*

Assume that FA of the phase element lies in TP of the polarizer in PUs of the radiation source and the photodetector, which means $\alpha'_j = \beta'$ in Eq. (17) and $\alpha_i = \beta$ in Eq. (22), and remains at this position as the polarizers rotate in the process of calibration. The Mueller matrix of PU with FA of the phase element lying in TP of the polarizer is equal to the Mueller matrix of the polarizer [14].

Let the angle φ be obtuse and the screen move from point 5 to point 6 (Fig. 1) along the axis Z. Set the angle $\beta' = \alpha'_j = 90^\circ$ in PU of the radiation source. Then the optical beam of the radiation source has the vector $\mathbf{S}_s$ given by Eq. (17) equal to

$$\mathbf{S}_s = (E, -E, 0,0)^T \quad (29)$$

for the radiation linearly polarized along the axis Y'.

The light flux $d\Phi_r^c$ incident on the photosensitive element of the photodetector

from the element dA of the screen surface A irradiated by the optical beam with the vector $\mathbf{S}_s$ given by Eq. (29) is equal to

$$d\Phi_r^c = C_1\beta(\gamma'')E\cos\gamma'\cos\gamma''dA/2\pi, \quad (30)$$

where C_1 is the coefficient equal to zero for the screen points not belonging to the volume $V_s(\varphi)$, γ' is the angle of incidence of the optical beam on the screen, γ'' is the angle between the normal to the surface A and the axis of the photodetector field of view, $\beta(\gamma'')$ is the coefficient β (Fig. 3) at the angle $\xi = \gamma''$, the coefficient 1/2 is equal to the attenuation of the nonpolarized radiation by the polarizer of the photodetector PU. At the angle $\gamma'' = 0$, the coefficient β is minimally dependent on the angle γ", and the angle γ' = π - φ, and therefore the angle γ" = 0 is optimal.

The light flux $d\Phi_r^c$ gives rise to the signal di_r^c at the photodetector output

$$di_r^c = C_2C_1\beta(\gamma'')\cos\gamma'\cos\gamma''EdA/2\pi,$$

where C_2 is the coefficient of photodetector sensitivity to the light flux from the source at the point of the element dA.

The integral signal i_r^c from the entire luminous surface A

$$i_r^c = \frac{\beta(\gamma'')\cos\gamma'\cos\gamma''}{2\pi}\iint_A C_1C_2EdA.$$

As the screen moves from point 5 to point 6 along the axis Z, the integral signal W_r^c is calculated as

$$W_r^c = \int_5^6 i_r^c dz = \frac{\beta(\gamma'')\cos\gamma'\cos\gamma''}{2\pi}\iiint_{V_s(\varphi)} C_1C_2Ed\nu, \quad (31)$$

where $d\nu = dAdz$..

The analogous conclusions can be also drawn for the diffusively transmitting screen (thin fluoroplastic sheet) at the angle 0° ≤ φ ≤ 10° [13].

If we remove the screen and irradiate the volume $V_s(\varphi)$ by the beam with the vector $\mathbf{S}_s$ given by Eq. (29), then the vector $d\mathbf{S}(i)$ of radiation scattered by the volume $d\nu(i)$ is

$$d\mathbf{S}(i) = \frac{E}{r(i)^2}(D_{11}-D_{12}, D_{21}-D_{22}, D_{31}-D_{32}, D_{41}-D_{42})^T d\nu(i),$$

and the vector $d\mathbf{S}_r(i)$ of radiation after photodetector PU at $\alpha_i = \beta = 0$ (polarizer TP is directed along the axis X) is

$$d\mathbf{S}_r(i) = \frac{E}{2r(i)^2}(D_{11}-D_{12}+D_{21}-D_{22}, D_{11}-D_{12}-D_{21}-D_{22}, 0, 0)^T d\nu(i).$$

The Stokes vector $d\mathbf{S}_r(i)$ corresponds to the luminous intensity

$$d\vec{I}_r(i) = \frac{E}{2}(D_{11}-D_{12}+D_{21}-D_{22})d\nu(i),$$

and the light flux $d\Phi_r(i)$ incident on the sensitive element of the photodetector is

$$d\Phi_r(i) = C_1d\vec{I}_r(i) = C_1\frac{E}{2}(D_{11}-D_{12}+D_{21}-D_{22})d\nu(i). \quad (32)$$

The light flux $d\Phi_r(i)$ described by Eq. (32) gives rise to the signal $i_r\uparrow^{\rightarrow}(i)$ at the photodetector output

$$i_r\uparrow^{\rightarrow}(i) = \frac{C_1C_2}{2}E(D_{11}-D_{12}+D_{21}-D_{22})d\nu(i). \quad (33)$$

The Stokes vector $d\mathbf{S}_r(i)$ of the radiation scattered by the volume element $d\nu(i)$ exposed to the incident radiation with the vector $\mathbf{S}_s$ described by Eq. (29) after PU of the photodetector with the polarizer TP along the axis Y is

$$d\mathbf{S}_r(i) = \frac{E}{2r(i)^2}(D_{11}-D_{12}-D_{21}+D_{22}, -D_{11}+D_{12}+D_{21}-D_{22}, 0, 0)^T d\nu(i).$$

This vector corresponds to the signal $i_r\uparrow\uparrow(i)$ at the photodetector output equal to

$$i_r\uparrow\uparrow(i) = \frac{C_1C_2E}{2}(D_{11}-D_{12}-D_{21}+D_{22})d\nu(i). \quad (34)$$

If we irradiate the volume $V_s(\varphi)$ by the optical beam with the Stokes vector $\mathbf{S}_s = (E,E,0,0)^T$ (the radiation is linearly polarized long the axis X') at the angle $\beta' = \alpha_i' = 0°$, then the Stokes vector $d\mathbf{S}(i)$ of the radiation scattered by the element $d\nu(i)$ is

$$d\mathbf{S}(i) = \frac{E}{r(i)^2}(D_{11}+D_{12}, D_{21}+D_{22}, D_{31}+D_{32}, D_{41}+D_{42})^T d\nu(i),$$

and the Stokes vector $d\mathbf{S}_r(i)$ of radiation after the photodetector PU with the polarizer TP along the axis X is

$$d\mathbf{S}_r(i) = \\ = \frac{E}{2r(i)^2}(D_{11}+D_{12}+D_{21}+D_{22}, D_{11}+D_{12}+D_{21}+D_{22}, 0, 0)^T d\nu(i).$$

The radiation with this Stokes vector corresponds to the signal $i_{r\rightarrow}^{\rightarrow}(i)$ at the photodetector output equal to

$$i_{r\rightarrow}^{\rightarrow}(i) = \frac{C_1C_2E}{2}(D_{11}+D_{12}+D_{21}+D_{22})d\nu(i). \quad (35)$$

The Stokes vector $d\mathbf{S}_r(i)$ of radiation scattered by the element $d\nu(i)$ after the photodetector PU with the polarizer TP along the axis Y is

$$d\mathbf{S}_r(i) = \\ = \frac{E}{2r(i)^2}(D_{11}+D_{12}-D_{21}-D_{22}, -D_{11}-D_{12}+D_{21}+D_{22}, 0, 0)^T d\nu(i).$$

The radiation with this Stokes vector corresponds to the signal $i_{r\rightarrow}\uparrow(i)$ at the photodetector output equal to

$$i_{r\rightarrow}\uparrow(i) = \frac{C_1C_2E}{2}(D_{11}+D_{12}-D_{21}-D_{22})^T d\nu(i). \quad (36)$$

Summing up the signals $i_r\uparrow^{\rightarrow}(i)$ (33), $i_r\uparrow\uparrow(i)$ (34), $i_{r\rightarrow}^{\rightarrow}(i)$ (35) and $i_{r\rightarrow}\uparrow(i)$ (36) from all elements $d\nu(i)$ of the volume $V_s(\varphi)$, we obtain the signal $i_{r\Sigma}$ equal to

$$i_{r\Sigma} = \iiint\limits_{V_s(\varphi)} (i_r\uparrow^{\rightarrow} + i_r\uparrow\uparrow + i_{r\rightarrow}^{\rightarrow} + i_{r\rightarrow}\uparrow)d\nu = \\ = \frac{D_{11}}{2}\iiint\limits_{V_s(\varphi)} C_1C_2Ed\nu. \quad (37)$$

Taking into account Eqs. (31) and (37), we obtain

$$D_{11} = \frac{i_{rD}\beta(\gamma'')\cos\gamma'\cos\gamma''}{\pi W_r^c}. \quad (38)$$

Substitute Eq. (38) into Eq. (27) and obtain the calibration coefficient

$$K(\varphi) = \frac{\pi W_r^c \tilde{D}_{11}}{i_{r\Sigma}\beta(\gamma'')\cos\gamma'\cos\gamma''}. \quad (39)$$

4. SOURCE OF RADIATION

The ideal source of radiation for polarization measurements should be monochromatic, have high spectral intensity, cover a wide spectral range, and have high directivity of radiation. **Fig. 4** shows the block diagram of a five-wave source of quasi-monochromatic radiation of high spectral intensity and directivity. The requirements for an ideal light source for polarization measurements can be met by a set of high-brightness LEDs with small size of luminous elements. High-brightness LEDs, whose main parameters are given in **Table 2**, are used as generators of radiation.

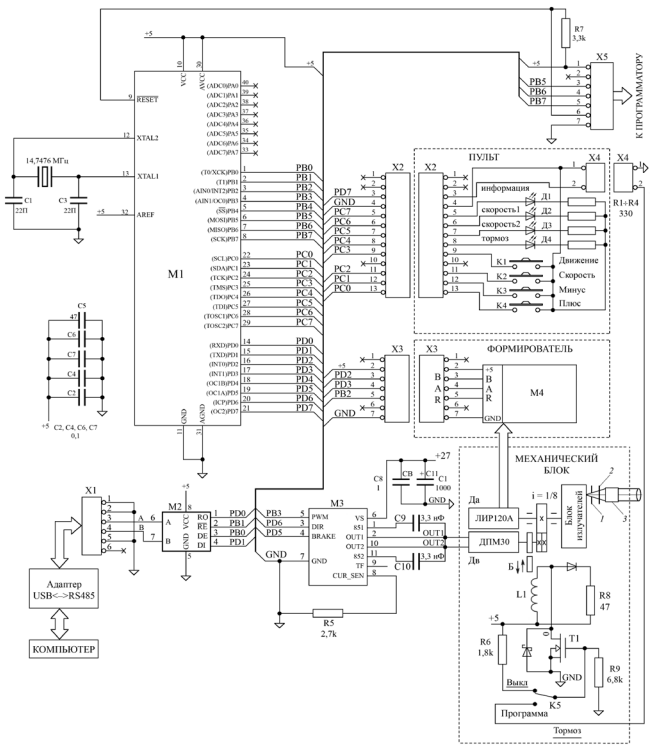

Fig. 4. *Block diagram of the source of radiation: Ø 0.5 diaphragm 1, depolarizer 2, GELIOS-44-2 objective 3, T1 – RLU120, M1– ATmega16, M2 – MAX 485, M3 – LMD18200.*

In the radiation source, LED with the diameter of the luminous element dle of 1 mm is set at a distance of 1 mm in front of the diaphragm 0.5

Table 2

Main LED parameters.

LED type	Color	λ_{rad}, nm	P_{rad}, W	U_{power}, V	I_{max}, mA	I_{av}, mA	δλ, nm/°C	d_{le}, mm
IPR169A9S	blue	455	0.6	3.5	700	350	0.17	1
IPR169A9L	green	525	0.3	3.5	700	350	0.17	1
IPR169A9Zh	yellow	555	0.15	2	700	350	0.17	1
IPR169A9Zh	orange	590	0.15	2	700	350	0.17	1
IPR169A9K	red	625	0.28	2	700	350	0.17	1

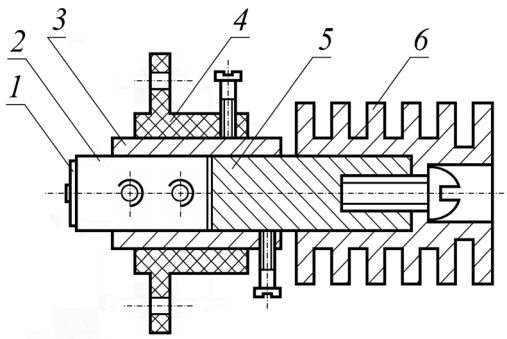

Fig. 5. *Block diagram of the emitter: LED 1, heatsink 2, cylinder 3, insulator 4, rod 5, and radiator 6.*

mm in diameter. The GELIOS-44-2 objective allows us to obtain the optical beam 25 mm in diameter with the divergence of 0.3°.

The minimal volume dv of clear air is equal to few cubic centimeters. We can take dr equal to 25 mm. Then the minimal volume is V_s (90°) in our case. It is possible to obtain more than 10 cm^3. The nephelometer base A = 1.2 m and A_r = 0.6 m can provide the measurement of the matrix D at φ_{min} = 1.8°. The optical beam parameter characterizing the error of approximation of the optical beam by the elementary optical beam varies from 0.0025 at φ = 90° to 0.013 at φ = 180°.

The emitter arrangement is shown in **Fig. 5.** LED 1 is soldered to heat sink 2 (copper plate 0.5 mm thick), which is clamped with screws in the groove of copper rod 5. Rod 5 moves longitu-dinally in copper cylinder 3. Cylinder 3 moves longitudinally in caprolon insulator 4. Radiator 6 increases the heat removal from LED. The power source of the LED D2 is an emitter voltage regu-lator on the transistor T1 (**Fig. 6**). As low voltage is applied to the input

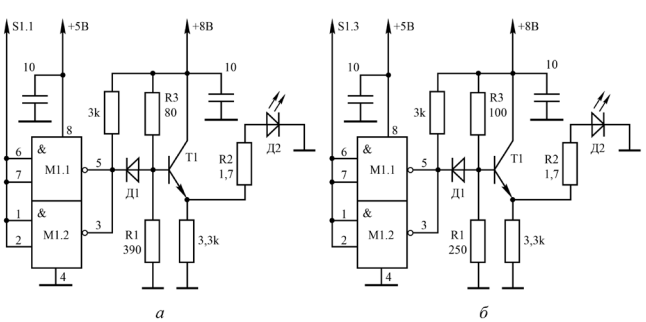

Fig. 6. *Power supply: a – 3.5 V; b – 2 V; M1 – 155LA18; T1 – SC3807; D1 – 1N4148.*

of the microcircuit M1, the voltage determined by the divider at resistors R1 and R3 is formed at the emitter of the transistor T1. Resistor R2 provides the negative feedback for stabilization of LED current. Resistor R2 is a constantan wire wound on an MLT (metal-film varnished heat-resistant)-type resistor.

The unit of emitters is a disk 150 mm in diameter turning around the axis. It comprises of five emitters placed in a circle (Fig. 5) and power sources (Fig. 6) blown from below by a micro-fan (**Fig. 7**). The required LED is placed against diaphragm 1 (Fig. 4) by the motor DV through a back-lash-free gearbox. Once the LED is set, the rotation of the disk with emitters and power supplies can be slowed down by the stop of the slider B on the rubberized disk. The angle of disk rotation around the axis is measured by the LIR120A transducer, which reflects it by the number of pulses with respect to the pulse R. Pulses B, A, and R from LIR120A come to the M4 shaper on the 555IP11 microcircuit and then through the X3 connector to the M1 AEmega16 microprocessor. The motor is controlled by the M3 LMD18200 driver. The program to the M1 microprocessor is saved through the X5 connector. The software of the M1 microcontroller accomplishes the function of a servo drive, in which the M3 LIR120A angle converter acts as a sensor, and the LDM18200 driver acts as a power bridge. The servo feedback operates by the principle of a PID

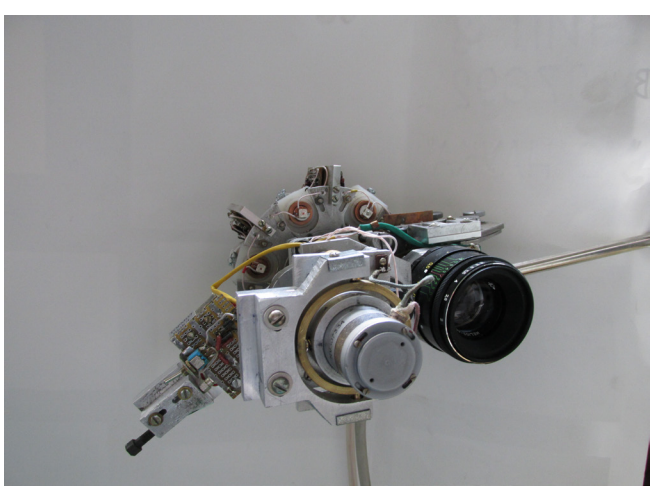

Fig. 7. *Source of radiation.*

(Proportional - Differential - Integral) controller, which calculates the speed and direction of movement depending on the difference between the current coordinate and the required one. In its turn, the required coordi-nate or, more exactly, the variable associated with it changes by the mathematical law during execu-tion of the movement command. This ensures a smooth start of the electric drive and its smooth de-celeration to zero speed at the finish point. The value of acceleration and deceleration of the electric drive is set by a separate variable in the microcontroller program. Smooth acceleration and decel-eration, as well as coordinate feedback with the PID controller, are provided by standard numerical control (CNC) mathematics.

The radiation source can be controlled both from a personal computer and from the control panel. Control commands from a personal computer are transferred through the X1 connector and the M2 MAX485 microcircuit.

The control panel allows the position of the emitter to be changed smoothly with three grada-tions of speed. High-speed gradation allows the drive to turn quickly to the needed angle. The low-speed gradation allows accurate adjustment of the emitter position. There is also a command for the initial setting of the emitter coordinate system with respect to the reference pulse of the output R of the LIR120A angle converter. The control panel also allows us to save the coordinate of a current position of the drive to the internal memory of the microcontroller to be able to return to this point at any time. The number of recorded positions can be up to five. With commands from the control panel, it is possible to move the drive to any of these recorded positions.

The PC control program has the same capabilities as the built-in control panel. In addition, with commands from the computer, it is possible to set the position of the emitter directly to the needed angle with the accuracy provided by the LIR120A angle converter (0.009°).

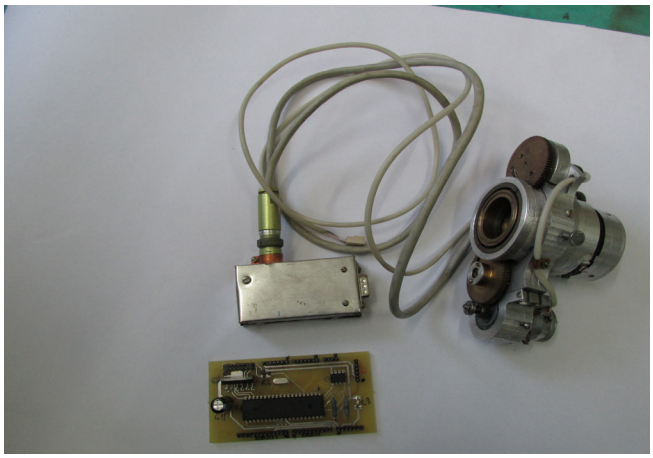

Fig. 8. *Polarization unit.*

A polarization unit (PU) can be connected in place of the mechanical unit (**Fig. 8**). The posi-tion of FA of the phase element of PU is controlled in the way similar to that described above.

The computer program allows up to five devices similar to the mechanical unit and PU to be controlled. It has three dialog tabs "Operation," "Settings," and "Port" (in **Fig. 9**). Two last tabs in-clude various settings, in particular, the communication port, positioning resolution (still identical for all axes of motion), and limiting speed. Figure 9 shows the dialog box of motion commands. In this window, one can see five horizontal arrays of keys and text fields arranged in one line. Each group of elements is associated with the control of one of five devices.

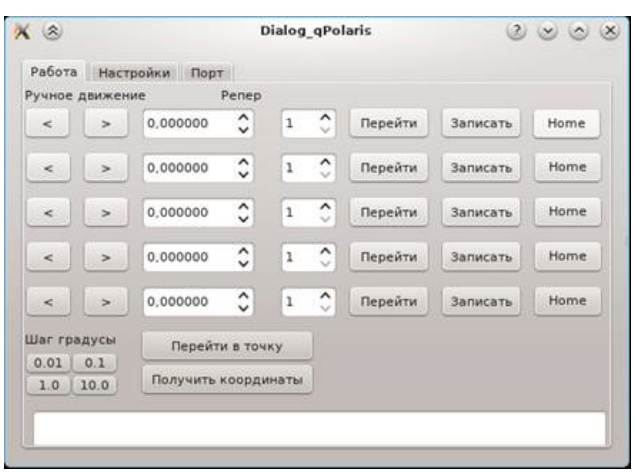

Fig. 9. *Example of operation of the software for control of five emitters.*

The computer program is written in C++ with the QtCreator version 4 open source software. This tool includes the free GCC-4.7 compiler and the popular Qt free interface library version 4. This solution opens the feasibility of not only writing programs with a modern user interface, but also compiling them for any platform, including Windows and Linux, for which there is a compiled Qt library on the Internet. Thus, the program can be compiled without changes even for most so-called embedded industrial computers, if they have the Qt-embedded 4.0 or 5.0 library.

5. CONCLUSIONS

The material presented in the paper allows one to determine the main parameters of a quasi-monochromatic radiation source of high spectral brightness being a component of a polarization nephelometer that measures matrix *D* in the range $\varphi = [\varphi_{min}, \varphi_{max}]$, as well as its design and operating principle. The external view of the polarization unit demonstrates the structure of the unit for high-precision control of the phase element.

REFERENCES

1. Rozenberg GV (ed.). *Searchlight Beam in the Atmosphere*. Moscow, AN SSSR Publ., 1960, pp. 146-174.
2. Oshlakov VG. Optimal measurer of the scattering phase matrix. *Optika atmosfery i okeana* [Atmospheric and oceanic optics], 1992, 5(11):767-769 (in Russ.).
3. Oshlakov VG, Borkov YuG. Numerical analysis of the instrumental matrix of a polarization meter. *Optika atmosfery i okeana* [Atmospheric and oceanic optics], 2002, 15(07):575-581 (in Russ.).
4. Gorchakov GI, Rozenberg GV. Measurement of the radiation scattering matrix in the atmospheric surface layer. *Izvestiya AN SSSR. Fizika atmosfery i okeana*, 1965, 1(12):1279-1287 (in Russ.).
5. Gorchakov GI. Matrices of radiation scattering by near-surface air. *Izvestiya AN SSSR. Fizika atmosfery i okeana,* 1966, 11(6):593-605 (in Russ.).
6. Sidorov VN. Flow-through polarization nephelometer. *Izvestiya AN SSSR. Fizika atmosfery i okeana,* 1979, 15(7):763-768 (in Russ.).
7. Lukshin VV, Isakov AA. Optical characteristics of smoke aerosols. *Izvestiya AN SSSR. Fizika atmosfery i okeana,* 1988, 24(3):250-257 (in Russ.).
8. Deirmendjian D. *Electromagnetic Scattering on Spherical Polydispersions*. RAND Corporation, Santa Monica, California, American Elsevier Publishing Company, New York, 1969.
9. Ivanov AP. *Optics of Scattering Media*. Moscow, Nauka i tekhnika Publ., 1969, 592 p.
10. Voevodin VV, Kuznetsov YuA. *Matrices and Calculations*. Moscow, Nauka Publ.,1984, 318 p.
11. Pritchard BS, Eliott WG. Two instruments for atmospheric optics measurements. *J. Opt. Soc. Am.,* 1960, 50(3):111.
12. Gurevich MM. *Photometry: Theory, Methods, and Devices*. Leningrad, Energoatomizdat Publ., 1983, 269 p.
13. Isakov AA. Study of atmospheric aerosol by the methods of radiation scattering at small angles. *Ph.D. Thesis*, Moscow, IFA AN Publ.,1979.
14. Gerrard A, Burch JM. *Introduction to Matrix Methods in Optics*. New York, Willey, 1975, 341 p.
15. Born M, Wolf E. *Principles of Optics*. London, Pergamon Press, 1959, 719 p.